

# Construction d'un modèle thermodynamique fiable et robuste pour les mélanges liquide-vapeur

P.M. Congedo, M.-G. Rodio, J. Tryoen, R. Abgrall

a. INRIA Bordeaux Sud-Ouest

## Résumé :

*La prédiction numérique des effets de transfert de masse dans les écoulements diphasiques est un outil fondamental dans plusieurs domaines. Un des problèmes est lié au traitement du mélange liquide-vapeur, notamment au niveau thermodynamique. Dans la littérature, on préfère en général utiliser des équations 'convexes', qui présentent une vitesse du son toujours réelle au-dessous de la courbe de saturation, comme par exemple, la 'Stiffened Gas (SG)'. Cependant, son utilisation dans la phase gaz ne garantit pas la prise en compte des effets de gaz réel, qui requièrent des lois beaucoup plus complexes généralement non-convexes. Cette étude se concentre sur la formulation d'un algorithme innovant de couplage fort entre un modèle de type SG et une équation d'état complexe quelconque pour la modélisation de la phase gazeuse, basé sur des données expérimentales. L'algorithme proposé sera basé sur un cadre bayésien, permettant la prise en compte d'incertitudes sur le modèle et les données.*

## Abstract :

*Numerical simulation of mass transfer in biphasic flows is a fundamental tool in various disciplines. One major issue is related to the thermodynamics of the liquid-vapor mixture. Usually, convex equations of state are used, where a real sound speed can be defined under the saturation curve, such as for example the Stiffened Gas (SG) equation. Nevertheless, the use of this equation in the gas phase, ban the prediction of real-gas effects, demanding a more complex equation of state, generally non-convex. The aim of this work is to formulate an innovative algorithm for a strong coupling between a SG equation and a whatever more complex equation for the gas phase, using experimental data. The proposed algorithm relies on a bayesian-based method, taking into account model and data uncertainties.*

**Mots clefs :** equations of state, biphasic flows, bayesian-based methods.

## 1 Introduction

Modeling two-phase flows is of primary importance for engineering applications. Two aspects are fundamental : (i) how to model the interface between two fluids with different thermodynamic properties and (ii) to characterize the mechanisms occurring at the interface as well as in zones where the volume fractions are not uniform. For several multiphase models, such as for example the discrete equation method (DEM), each phase is compressible and behaves according to a convex equation of state (EOS). In many works of interface problem, the *Stiffened Gas* (SG) EOS was usually used [3, 9]. As explained in Saurel *et al.* [11], this EOS allows an explicit mathematical calculations of important flow relation thanks to its simple analytical form. Moreover, in mass transfer problem it assures the positivity of speed of sound in the two-phase region, under the saturation curve.

When complex fluids are considered, such as cryogenic and BZT fluid, molecularly complex and so on, the use of simple EOS can produce imprecise estimation of the thermodynamic properties, thus deteriorating the accuracy of the prediction. Increasing the complexity of the model and calibrating the adding parameters with respect to the available experimental data constitutes a valid option for saving the good prediction of the model. Nevertheless, it could be very challenging because of the

numerical difficulties for the implementation of more complex mathematical model and because of the large uncertainties that generally affected the experimental data.

An effort for developing a more predictive tool for multiphase compressible flows is underway in Bacchus Team (INRIA-Bordeaux). Within this project, several advancements have been performed, *i.e.* considering a more complete systems of equations including viscosity [2], working on the thermodynamic modeling of complex fluids [5, 6], and developing stochastic methods for uncertainty quantification in compressible flows [5, 1]. The aim of this paper is to show how a complex thermodynamics can be handled in a liquid-vapor mixture in a bayesian framework.

In this paper, two thermodynamic models are considered, *i.e.* the SG EOS and the Peng-Robinson (PRSV) EOS. While SG allows preserving the hyperbolicity of the system also in spinodal zone, real-gas effects are taken into account by using the more complex PRSV equation. The higher robustness of the PRSV equation when coupled with CFD solvers with respect to more complex and potentially more accurate multi-parameter equations of state has been discussed in [4, 7]. In this paper, the PRSV equation is used only to describe the vapor behavior, while the SG model is used for describing the liquid-vapor mixture using experimental data and synthetic data from PRSV equation. In practice, the coefficients of the SG equation are calibrated for obtaining a saturation curve closed to the experimental one and to the PRSV saturation curve. This paper is organized as follows. In section 2, both SG and PRSV models are described. Section 4 illustrated the calibration of SG with respect to the experimental data and to PRSV equation for the dodecane and the D6 fluid.

## 2 Description of thermodynamic models

As we have previously mentioned, we deal with pure fluid and artificial mixture zone, thus the EOS must be able to describe the flow both in pure fluids and mixture zones.

In this section, first we describe two EOSs, *i.e.* the Stiffened Gas (SG) EOS and the Peng-Robinson (PR) EOS. Then, we build the mixture EOS using first the SG EOS for each phase and after the PR and the SG for the gas and the liquid phase, respectively.

### 2.0.1 Stiffened Gas EOS for pure fluid

The Stiffened Gas EOS is usually used for shock dynamics and its robustness for simulating two-phase flow with or without mass transfer has been amply demonstrated [3]. It can be written as follows :

$$P(\rho, e) = (\gamma - 1)(e - q)\rho - \gamma P_\infty, \quad (1)$$

$$e(\rho, T) = Tc_v + \frac{P_\infty}{\rho c_v} + q \quad (2)$$

$$h(T) = \gamma c_v T, \quad (3)$$

where  $p$ ,  $\rho$  and  $e$  are the pressure, the density and the energy, respectively. The politropic coefficient  $\gamma$  is the constant ratio of specific heat capacities  $\gamma = c_p/c_v$ ,  $P_\infty$  is a constant reference pressure and  $q$  is the energy of the fluid at a given reference state. Moreover,  $T$ ,  $c_v$  and  $h$  are the temperature, the specific heat at constant volume and the enthalpy, respectively. The speed of sound, defined as  $c^2 = (\frac{\partial P}{\partial \rho})_s$  can be computed as follows :

$$c^2 = \gamma \frac{P + P_\infty}{\rho} = (\gamma - 1)c_p T \quad (4)$$

where  $c^2$  remains strictly positive (for  $\gamma > 1$ ). It ensures the hyperbolicity of the system and the existence of a convex mathematical entropy.

The procedure to build the saturation curve for a liquid-phase mixture is illustrated in [11] and it is based on the imposition of the phase chemical potentials (Gibbs function) equality. The chemical potential formulation for each phase is defined as follows :

$$G_l(P, T) = (\gamma_l C_{v,l} - q_l')T - C_{v,l}T \ln \frac{T^{\gamma_l}}{(P + P_{\infty,l})^{\gamma_l - 1}} + q_l \quad (5)$$

$$G_g(P, T) = (\gamma_g C_{v,g} - q'_g)T - C_{v,g}T \ln \frac{T^{\gamma_g}}{(P + P_{\infty,g})^{\gamma_g - 1}} + q_g, \quad (6)$$

where  $q'$  is a constant. The saturation curve is obtained by imposing that  $G_l$  is equal to  $G_g$ , thus yielding the following equation :

$$\ln(P + P_{\infty,g}) = A + \frac{B}{T} + C \ln T + D \ln(P + P_{\infty,l}), \quad (7)$$

where,

$$A = \frac{C_{p,l} - C_{p,g} + q'_g - q'_l}{C_{p,g} - C_{v,g}}, \quad B = \frac{q_l - q_g}{C_{p,g} - C_{v,g}}, \quad C = \frac{C_{p,g} - C_{p,l}}{C_{p,g} - C_{v,g}}, \quad D = \frac{C_{p,l} - C_{v,l}}{C_{p,g} - C_{v,g}}. \quad (8)$$

Since the focus in this paper is on the SG parameters to calibrate, the following ones will be treated in a bayesian framework :  $P_{\infty,l}$ ,  $C_{p,l}$ ,  $C_{p,g}$ ,  $C_{v,l}$ ,  $C_{v,g}$ ,  $q_l$ ,  $q_g$ , and  $q'_g$ . According to [11], it is assumed that parameters  $P_{\infty,g}$  and  $q'_l$  are equal to zero.

### 2.0.2 Peng-Robinson (PRSV) EOS for pure fluid

The Peng-Robinson-Strijek-Vera (PRSV) cubic equation of state (EoS) is adopted for this study in order to describe the thermodynamic behavior of real gas :

$$p = \frac{RT}{v - b} - \frac{a}{v^2 + 2bv - b^2}. \quad (9)$$

where  $p$  and  $v$  denote respectively the fluid pressure and its specific volume,  $a$  and  $b$  are substance-specific parameters related to the fluid critical-point properties  $p_c$  and  $T_c$  and representative of attractive and repulsive molecular forces. To achieve high accuracy for saturation-pressure estimates of pure fluids, the temperature-dependent parameter  $a$  in Eq. (9) is expressed as

$$a = (0.457235R^2T_c^2/p_c) \cdot \alpha(T), \quad (10)$$

while

$$b = 0.077796RT_c/p_c. \quad (11)$$

The correction factor  $\alpha$  in Eq. (10) is given by

$$\alpha(T_r) = [1 + K(1 - T_r^{0.5})]^2, \quad (12)$$

with

$$K = 0.378893 + 1.4897153\omega - 0.17131848\omega^2 + 0.0196554\omega^3. \quad (13)$$

The parameter  $\omega$  is the fluid acentric factor. The other needed information to complete the thermodynamic model, namely the ideal-gas isochoric specific heat of the fluid, is approximated through a power law, *i.e.*,

$$c_{v,\infty}(T) = c_{v,\infty}(T_c) \left(\frac{T}{T_c}\right)^n \quad (14)$$

with  $n$  a fluid-dependent parameter.

## 3 Bayesian Framework

We propose a methodology for calibrating the SG coefficients based on a Bayesian setting, that is, probability densities of plausible values of these coefficients are rebuilt from couples of temperature and pressure of saturation curves. A Bayesian setting offers a rigorous foundation for inferring model parameters from data, a natural mechanism for incorporating prior information, and a quantitative assessment of uncertainty on the inferred results [10]. The output of Bayesian inference is not a single

value for the model parameters, but a posterior probability distribution that summarizes all available information about parameters. From this distribution, one can calculate moments, compute marginal distributions, or make additional predictions by averaging over the posterior.

Let  $\mathbf{m}$  denote the vector of SG coefficients  $\mathbf{m} = (P_{\infty,l}, C_{p,l}, C_{p,g}, C_{v,l}, C_{v,g}, q_l, q_g, q'_g)$  and  $F$  the mathematical model derived from (3) defined as follows :  $P = F(\mathbf{m}, T)$ , which yields predictions of the pressure as a function of the temperature and the SG coefficients. In practice, it consists in a non-linear problem, which is solved here using a classical Newton-Raphson algorithm. In the Bayesian setting, the components of  $\mathbf{m}$  are random variables and we use Bayes' rule to define a posterior probability density for the model parameters  $\mathbf{m}$ , given  $n$  observations of temperature/pressure couples  $\{\mathbf{d}^1, \dots, \mathbf{d}^n\} = \{(P^1, T^1), \dots, (P^n, T^n)\}$  :

$$p(\mathbf{m}|\mathbf{d}^1, \dots, \mathbf{d}^n) = \frac{p(\mathbf{d}^1, \dots, \mathbf{d}^n|\mathbf{m})p_{\mathbf{m}}(\mathbf{m})}{\int p(\mathbf{d}^1, \dots, \mathbf{d}^n|\mathbf{m})p_{\mathbf{m}}(\mathbf{m})d\mathbf{m}}. \quad (15)$$

Prior probability  $p_{\mathbf{m}}(\mathbf{m})$  represents the degree of belief about possible values of  $\mathbf{m}$  before observing any data ; non-informative uniform priors are here used, with intervals of plausible values depending on the fluid. Data then enters the formulation through the likelihood or joint density of the observations given  $\mathbf{m}$ , namely  $p(\mathbf{d}^1, \dots, \mathbf{d}^n|\mathbf{m})$ . A common model assumes independent observations so that independent additive errors account for the deviation between predicted and observed values of  $\mathbf{d}$  :

$$P^j = F(\mathbf{m}, T^j) + \eta^j, \quad j = 1, \dots, n. \quad (16)$$

A typical assumption is that errors are realizations of a Gaussian random variable  $\eta^j \sim \mathcal{N}(0, \sigma^2)$ ,  $\sigma$  encompassing model and data errors. In that case,  $P^j|\mathbf{m} \sim \mathcal{N}(F(\mathbf{m}, T^j), \sigma)$ , and the likelihood is

$$p(\mathbf{d}^1, \dots, \mathbf{d}^n|\mathbf{m}) = \prod_{j=1}^n p_{\mathbf{d}^j}(\mathbf{d}^j|\mathbf{m}) = \prod_{j=1}^n p_{\eta}(P^j - F(\mathbf{m}, T^j), \sigma^2), \quad (17)$$

with  $p_{\eta}$  the Gaussian density probability of  $\mathcal{N}(0, \sigma^2)$ . Since in general model and data errors are not known with exactness, one considers  $\sigma$  as an hyper-parameter of the Bayesian setting that needs to be inferred, with noninformative uniform a priori. However, one has to take into account the different scales of pressure, so that  $\sigma$  depends on temperature. In practice, data are assembled five by five, the pressure mean  $\mu^k$  is computed for each package, and one infers  $e = \sigma^k/\mu^k$ .

Markov Chain Monte Carlo (MCMC) encompasses a broad class of methods that simulate drawing samples from the normalized posterior [8] :

$$p(\mathbf{m}, e|\mathbf{d}^1, \dots, \mathbf{d}^n) \propto p(\mathbf{d}^1, \dots, \mathbf{d}^n|\mathbf{m}, e)p_{\mathbf{m}}(\mathbf{m})p_e(e), \quad (18)$$

thus avoiding complex numerical integrations in high dimensions to form the posterior distribution. In this work, we use the Metropolis-Hastings algorithm with single-site updating and Gaussian proposal density to draw samples of  $p(\mathbf{m}, e|\mathbf{d}^1, \dots, \mathbf{d}^n)$  with an adaptation of the proposal distribution widths in the first iterations [12].

## 4 Results

This section illustrates various results. First, the SG coefficients are calibrated with respect to the experimental data for the dodecane fluid. Secondly, the SG is calibrated considering the saturation curve generated by means of PRSV equation, thus providing a practical and efficient way for coupling PRSV and SG. Finally, the same procedure is applied for a complex gas, *i.e.* the D6, that displays BZT [5] properties close to the saturation curve. In this case, the calibrated SG features to allow the simulation of a liquid-vapor mixture for a very complex gas.

Marginal posterior distributions of the SG coefficients for the first case are reported in Figure 1, while posterior means, coefficients of variation (standard deviation - denoted by std in the following - to mean ratio), and 90% confidence intervals are reported for the three cases in Table 1. Multi-modal

distribution of the various coefficients are due to numerical non-linear interactions since each coefficient has no more a precise physical meaning. One can denote that the reconstruction for all SG coefficients except  $P_{\infty,l}$  are really stable ( $\text{std}/\text{mean} \leq 2\%$ ), while the error on  $P_{\infty,l}$  vary between 6% and 15%. This may be explained by the presence of another solution that is plausible, although less accurate.

Finally, SG saturation curves are plotted in Figure 2 for the different test cases, using the means of the different coefficients. The curves obtained are observed to fit very well to the experimental data, and a comparison of the curve with the one obtained by [11] for the dodecane is given in the first panel. Note that the calibrated SG can reproduce very accurately the D6 saturation curve, providing a practical and efficient way for coupling SG and PRSV for a very molecularly complex fluid. Ongoing effort consists in a more accurate analysis of the variation of the thermodynamic properties when changing the equation and in the implementation of the calibrated SG in a CFD code.

## Références

- [1] Abgrall, R., Congedo, P.M. 2013 A semi-intrusive deterministic approach to uncertainty quantifications in non-linear fluid flow problems *J. Comput. Phys.* **235** 828-845

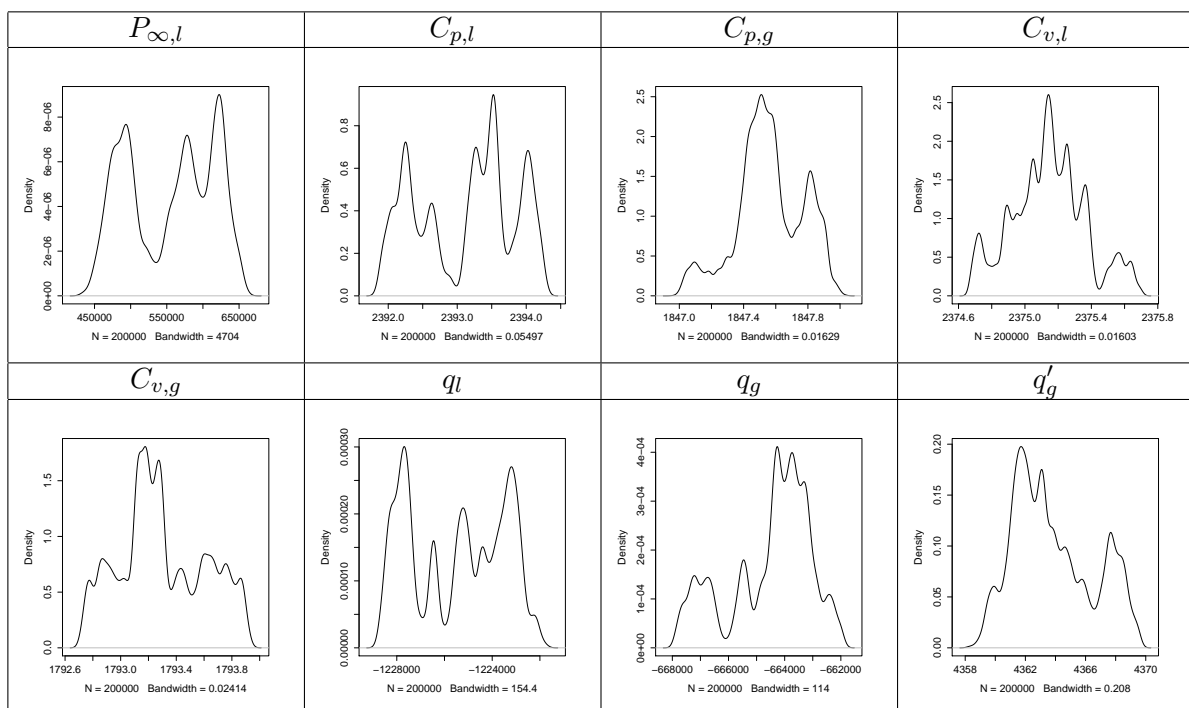


FIGURE 1 – Posterior probability densities of the SG-EXP coefficients

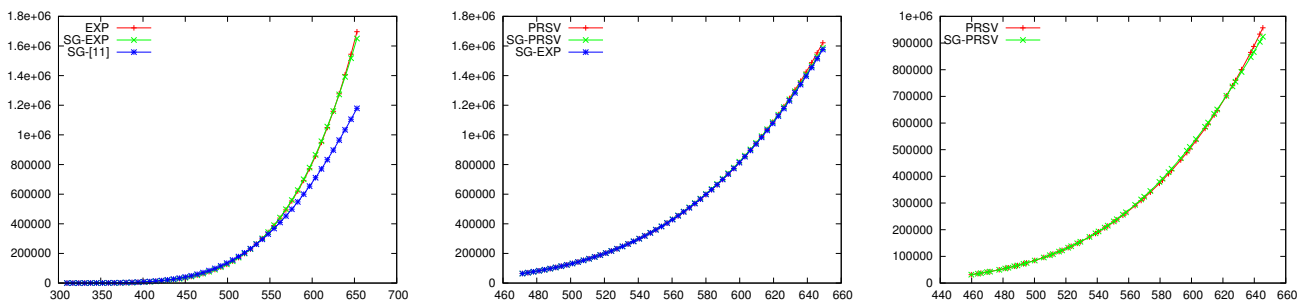


FIGURE 2 – SG saturation curves for dodecane calibrated with respect to experimental data (left) and PRSV data (middle). SG saturation curve for D6 calibrated with respect to PRSV data (right).

|                          |                | EXP<br>dodecane                                | PRSV<br>dodecane                               | PRSV<br>D6                                     |
|--------------------------|----------------|--|--|--|
| mean                     | $P_{\infty,l}$ | $5.548496 \times 10^5$                         | $4.495920 \times 10^5$                         | $2.715075 \times 10^5$                         |
|                          | $C_{p,l}$      | $2.393128 \times 10^3$                         | $2.395066 \times 10^3$                         | $1.011353 \times 10^3$                         |
|                          | $C_{p,g}$      | $1.847559 \times 10^3$                         | $1.848796 \times 10^3$                         | $6.115449 \times 10^2$                         |
|                          | $C_{v,l}$      | $2.375144 \times 10^3$                         | $2.377901 \times 10^3$                         | $9.960849 \times 10^2$                         |
|                          | $C_{v,g}$      | $1.793296 \times 10^3$                         | $1.793832 \times 10^3$                         | $5.875065 \times 10^2$                         |
|                          | $q_l$          | $-1.225480 \times 10^6$                        | $-1.235067 \times 10^6$                        | $-3.465248 \times 10^5$                        |
|                          | $q_g$          | $-6.645063 \times 10^5$                        | $-6.714408 \times 10^5$                        | $-3.330867 \times 10^4$                        |
|                          | $q'_g$         | $4.363827 \times 10^3$                         | $4.394854 \times 10^3$                         | $2.788734 \times 10^3$                         |
|                          | $e$            | $7.621892 \times 10^{-3}$                      | $6.979583 \times 10^{-3}$                      | $1.218782 \times 10^{-2}$                      |
|                          | std/mean       | $P_{\infty,l}$                                 | $1.082 \times 10^{-1}$                         | $1.556 \times 10^{-1}$                         |
| $C_{p,l}$                |                | $2.932 \times 10^{-4}$                         | $4.926 \times 10^{-4}$                         | $3.917 \times 10^{-4}$                         |
| $C_{p,g}$                |                | $1.126 \times 10^{-4}$                         | $1.812 \times 10^{-4}$                         | $5.153 \times 10^{-4}$                         |
| $C_{v,l}$                |                | $9.335 \times 10^{-5}$                         | $9.881 \times 10^{-5}$                         | $1.91 \times 10^{-4}$                          |
| $C_{v,g}$                |                | $1.718 \times 10^{-4}$                         | $2. \times 10^{-4}$                            | $2.454 \times 10^{-4}$                         |
| $q_l$                    |                | $1.608 \times 10^{-3}$                         | $3.129 \times 10^{-3}$                         | $1.129 \times 10^{-3}$                         |
| $q_g$                    |                | $2.199 \times 10^{-3}$                         | $1.843 \times 10^{-3}$                         | $2.325 \times 10^{-2}$                         |
| $q'_g$                   |                | $6.084 \times 10^{-4}$                         | $6.303 \times 10^{-4}$                         | $6.934 \times 10^{-4}$                         |
| $e$                      |                | $1.761 \times 10^{-1}$                         | $3.505 \times 10^{-1}$                         | $2.648 \times 10^{-1}$                         |
| 90% confidence intervals |                | $P_{\infty,l}$                                 | $[4.647 \times 10^5, 6.372 \times 10^5]$       | $[3.298 \times 10^5, 5.274 \times 10^5]$       |
|                          | $e$            | $[5.698 \times 10^{-3}, 9.998 \times 10^{-3}]$ | $[4.346 \times 10^{-3}, 1.183 \times 10^{-2}]$ | $[8.462 \times 10^{-3}, 1.882 \times 10^{-2}]$ |

TABLE 1 – Posterior means, variation coefficients, and 90% confidence intervals of the SG coefficients and of the model/data error parameter calibrated with respect to different data

- [2] Abgrall, R., Rodio, M.-G. 2012 Asymptotic Expansion of a Multiscale Numerical Scheme for Compressible Viscous Multiphase Flows *INRIA RR7920*
- [3] Abgrall, R., Saurel, R. 2003 Discrete Equations for Physical and Numerical Compressible Multiphase Mixtures *J. Comput. Phys.* **186** 361-396
- [4] Cinnella, P., Congedo, P.M., Pediroda, V., Parussini, L. 2010 Quantification of thermodynamic uncertainties in real gas flows *IJESMS* **2** 12-24
- [5] Cinnella, P., Congedo, P.M., Pediroda, V., Parussini, L. 2011 Sensitivity analysis of dense gas flow simulations to thermodynamic uncertainties *Phys. Fluids* **23** 116101
- [6] Congedo, P.M., Colonna, P., Corre, C., Witteveen, J.A.S., Iaccarino, G. 2012 Backward uncertainty propagation method in flow problems : Application to the prediction of rarefaction shock waves *Comput. Methods in Appl. M.* **213** 314-326
- [7] Congedo, P.M., Corre, C., Martinez, J.-M. 2011 Shape Optimization of an Airfoil in a BZT Flow with Multiple-source Uncertainties *Comput. Methods in Appl. M.* **200** 216-232
- [8] Gilks, W.R., Richardson, S., Spiegelhalter, D.J. 1996 Markov Chain Monte Carlo in Practice.
- [9] Goncalves, E., Patella, R.F. 2009 Numerical simulation of cavitating flows with homogeneous models *Computers and Fluids* **38** 1682-1696
- [10] Kaipio, J., Somersalo, E. 2010 Statistical and Computational Inverse Problems. *Applied Mathematical Sciences, Vol. 160 (ed. Springer)*
- [11] Le Metayer, O., Massoni, J., Saurel, R. 2004 Elaborating equations of state of a liquid and its vapor for two flow models. *International Journal of Thermal Sciences* **43** 265-276
- [12] Roberts, G.O., Rosenthal, J.S. 2006 Examples of adaptive MCMC *Stat. and Comput*